

Comments on the Defect Chemistry of Magnesium-Doped Lithium Niobate (LiNbO₃)

H. Donnerberg

FB Physik, University of Osnabrück, D-49069 Osnabrück, Germany

Received November 6, 1995; in revised form January 29, 1996; accepted January 31, 1995

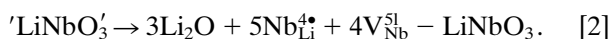
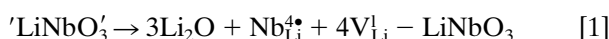
Congruently grown LiNbO₃ is known to be highly defective due to its significant Li₂O deficiency. At present two stoichiometry-related defect-chemical models are discussed which can be distinguished with respect to the occurrence of Li or Nb vacancies. The Nb-vacancy model takes advantage of ilmenite-structured LiNbO₃ and predicts a niobium antisite concentration being at least five times as large as in the Li-vacancy model. In the present contribution it is argued that the magnesium-doping mechanisms are essentially independent of these particular differences. It is argued that extended stoichiometry-related defect clusters represent a key for a proper understanding of the defect chemistry of impurity cations. The discussion is mainly based on our recent shell-model simulations of perfect and defective LiNbO₃. © 1996 Academic Press, Inc.

INTRODUCTION

The photorefractive properties of Li₂O-deficient LiNbO₃ are subject to drastic changes upon doping this material with magnesium. Whereas the photorefractive effect is useful for the storage of volume phase holograms, it is unwanted in optical waveguides. Zhong *et al.* (1) have discovered that this optical damage is significantly reduced in crystals grown from a congruent melt containing at least 4.6 mol% MgO. Several physical crystal properties show abrupt changes when the MgO content is raised above this threshold concentration. It is noticeable that analogous effects can be observed by keeping the Mg content fixed and varying instead the [Li]/[Nb] ratio (2, 3). Thus Mg cations only indirectly influence the threshold behavior by their solution modes which seem to be highly correlated with the stoichiometry-related, intrinsic defect structures in LiNbO₃. Therefore, in order to properly understand the incorporation of magnesium over the whole solution range one must first consider the existing stoichiometry-related intrinsic defects.

In the past different models have been proposed in order to describe the accommodation of Li₂O deficiency in LiNbO₃. In what follows we may omit the discussion of the model related to oxygen vacancies (4) since this contra-

dicts the observed density changes upon increasing the nonstoichiometry. The two remaining models consider all compensating defects to occur on the cationic sublattices:



I have used the Kröger–Vink notation (5) to formulate these chemical solid-state reactions. In addition, ${}^{\prime}\text{LiNbO}_3'$ denotes the whole bulk of perfectly grown LiNbO₃. Model [1] corresponds to the chemical sum formula Li_{1-4x}Nb_{1+x}O₃ and model [2] to (Li_{1-5x}Nb_{5x})Nb_{1-4x}O₃.

The most obvious difference between reactions [1] and [2] relates to the concentration of niobium antisite defects (Nb_{Li}^{4•}) and to the occurrence of Li or Nb vacancies. The earlier X-ray analysis of Abrahams and Marsh (6) strongly supported the Nb-vacancy model; further evidence was given by NMR-investigations of Peterson and Carnevale (7) and, later, by Hu *et al.* (8). These experimental data suggested an antisite concentration on the order of 5–6 mol% in congruently grown LiNbO₃. Such an amount is incompatible with the defect model (1) which ends up with 1 mol% Nb_{Li}^{4•}. However, the recent structure investigations of Iyi *et al.* (9) and Wilkinson *et al.* (10) based on sensitive neutron diffraction techniques favored the Li-vacancy model (1). Noticeably the NMR studies of Blümel *et al.* (11) are in agreement with these structural analyses. Blümel *et al.* point out that certain experimental inadequacies would have caused the artificial second Nb signal which has been observed in the earlier NMR experiments.

Based on the recently gained experimental information one is inclined to favor the Li-vacancy model (1), however, the ultimate proof is still lacking. It seems not unambiguously clear which of the two models correctly describes the intrinsic defect chemistry of LiNbO₃ related to the observed nonstoichiometry. It might be possible that both models are correct to some extent, since the detailed growth conditions could influence nature's choice of the

particular reaction. However, there are no investigations on this topic.

Recently we published our extensive atomistic computer simulations of possible defect structures in LiNbO_3 (12, 13). For the computational details I refer to these references and for further methodological questions to the review on solid-state simulations edited by Catlow and Mackrodt (14). For the present purposes it suffices to summarize the basic ideas underlying these simulations. Our method was based on static lattice energy minimization techniques which have been extensively employed in many studies of defect formations in insulating materials. There are now numerous examples of successful investigations of complex oxides including BaTiO_3 (15), KNbO_3 (16, 17), KTaO_3 (18), garnets (19, 20), and also high- T_C superconductors (e.g., Refs. (21, 22)). All corresponding simulations employ potential models based on interatomic pair-potentials of the Born-model type with formal (integral) ion charges and analytical short-range potentials of the Buckingham form:

$$V(r) = A \exp(-r/\rho) - C/r^6. \quad [3]$$

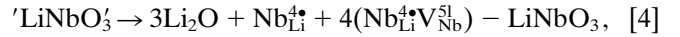
In addition, a shell-model treatment is included to simulate electronic polarizability contributions. Potential and shell parameters appropriate for LiNbO_3 have been obtained either from simulation studies of the binary oxides Li_2O and Nb_2O_5 or from direct fitting to structural, elastic, and dielectric properties of LiNbO_3 . On the basis of these potential simulations of LiNbO_3 it has been possible to calculate the formation energies of intrinsic and extrinsic point defects or even small defect clusters. The accompanying defect-induced lattice deformations have been fully taken into account. The combination of basic defect formation energies according to the various solid-state reactions accomplished the determination of (internal) reaction energies which have been further used to judge on the chemical relevance of possible defect structures. I emphasize that all employed potential models provided consistent qualitative predictions of defect structures in LiNbO_3 which underlines the reliability of our investigations. Moreover, entropy terms ($-T \cdot s$) which had been neglected may be expected to represent only small corrections in comparison with the internal energies (u) even at elevated temperatures. Therefore, the dominating contributions to the free energies $f = u - Ts$ of defect formation are given by the internal formation energies. This is suggested by corresponding investigations of some fundamental defect formations in alkali halides and magnesium oxide (23).

The first section is devoted to a brief review of stoichiometry-related defects which is followed by a detailed discussion of the magnesium incorporation. It is argued that the corresponding impurity solution model is essentially independent of the specific differences between the underlying nonstoichiometry defect models as far as one assumes

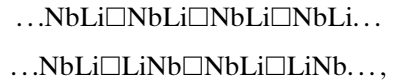
the existence of extended intrinsic defect clusters. Computer simulations as well as experimental results indicate that this assumption is realistic. On the other hand, solution models based on isolated stoichiometry-induced defects are believed to fail in accounting for the relevant experimental observations. The recently proposed solution model of Iyi *et al.* (24) belongs to this latter category.

COMMENTS ON STOICHIOMETRY-RELATED DEFECT MODELS

First, I briefly survey the two Li_2O -deficiency models based on Eqs. [1] and [2]. Of course, the first model is appealing because of its simplicity. Different from Eq. [2] it involves only a comparatively small number of highly charged defects which render model [1] energetically favorable. Our earlier computer simulations show that the energy difference between both models amounts to 11 eV per lost Li_2O molecule. In order to satisfy the experimental results of Abrahams and Marsh (6), Smyth (25) proposed the formation of appropriate defect clusters. Starting with the reaction



which immediately follows from Eq. [2] by a few rearrangements, Smyth observed that the defect complexes ($\text{Nb}_{\text{Li}}^{4+}\text{V}_{\text{Nb}}^{5-}$) may be interpreted as basic Li vacancies within ilmenite-structured LiNbO_3 , because perfect and ilmenite-structured LiNbO_3 differ only by their cation stacking sequence along the crystallographic c axis, i.e.,



respectively. In this representation \square denotes a structural cation vacancy. The Li vacancies would be related to the LiNb units. A necessary condition of this model to become favorable is that perfectly grown LiNbO_3 and ilmenite-structured LiNbO_3 are energetically almost equivalent. Indeed, our previous shell-model simulations yielded an energy difference between both structural modifications of 0.1 eV per unit cell which only slightly prefers the perfect LiNbO_3 . This value is in excellent agreement with recent calorimetric measurements by Mehta *et al.* (26). On the basis of these theoretical and experimental results it seems possible that both crystal structures exist within the same bulk as is commonly grown from a melt.

Supposing that the results of Abrahams and Marsh are correct, one must assume that all possible ilmenite-structured intergrowths are massively Li depopulated. This is due to the observation that reaction [4] accounts for almost all occurring Nb-antisite defects. Additional ilmenite-

structured, but stoichiometric regions would lead to surplus antisite defects being independent of Eq. [4] and, therefore, the total antisite concentration should significantly exceed the observed 5–6%. Stated in another way, this discussion suggests the formation of large clusters consisting of intrinsic, stoichiometry-related defects possessing a structure which resembles the ilmenite modification.

However, it is important to realize that defect clustering may analogously be expected on the basis of the model Eq. [1] as this would similarly allow to effectively screen the charges of the antisite defects and, therefore, to reduce defect-induced lattice strains. Support in favor of this suggestion is given by simulations of basic aggregations between Nb antisites and Li vacancies: In comparison with completely isolated point defects the formation of a neutral $\text{Nb}_{\text{Li}}^{4+}\text{-}4\text{V}_{\text{Li}}^1$ defect complex is stabilized by 1.65 eV. The dissociation of one Li vacancy requires at least 0.3 eV which indicates that stoichiometry-related vacancies are likely to be attracted by the existing antisites. The stability of these defect clusters may probably be further enhanced by suitable agglomerations of many $\text{Nb}_{\text{Li}}^{4+}\text{-}4\text{V}_{\text{Li}}^1$ complexes. However, it is beyond the range of our simulation techniques to determine the optimum size and shape of stoichiometry-related defect clusters.

Consequently, the ultimate difference between Eqs. [1] and [2] concerns only the structure of the proposed defect clusters, i.e., the precise way of the agglomeration of vacancies and of Nb cations. The comparison of lattice energies of perfect and ilmenite-type LiNbO_3 suggests that both types of cluster formations might be almost equally favorable (this corresponds to a “large-scale limit” of defect cluster sizes). A similar conclusion follows by considering “small-scale” cluster formations, i.e., $(\text{Nb}_{\text{Li}}^{4+}\text{V}_{\text{Li}}^1)$ and $(\text{Nb}_{\text{Li}}^{4+}(\text{V}_{\text{Nb}}^1\text{Nb}_{\text{Li}}^{4+}))$. Whereas in the first situation the stabilization energy is -0.7 eV, it equals -2.4 eV in the second case. In these simulations vacancies (V_{Li}^1 or $(\text{V}_{\text{Nb}}^1\text{Nb}_{\text{Li}}^{4+})$) and Nb antisites have been assumed on nearest possible lattice positions. Thus, the formation of sufficiently extended intrinsic defect clusters is not only able to lower the total reaction energies but significantly reduces also the energy difference between Eqs. [1] and [2]. Consequently, it cannot be ruled out that the proper choice between both models might depend on the actual crystal growth conditions. Of course, this speculation calls for further clarifying experimental investigations.

In conclusion, computer simulations indicate that it is energetically favorable to form defect clusters consisting of the stoichiometry-related Nb antisites and cation vacancies. This is expected to be true irrespective of the underlying defect model, i.e., [1] or [2]. It may be speculated that the relevant defect clusters consist of many $\text{Nb}_{\text{Li}}^{4+}\text{-}4\text{V}_{\text{Li}}^1$ units and are therefore extended in space (V_{Li}^1 represents either V_{Li}^1 or $(\text{V}_{\text{Nb}}^1\text{Nb}_{\text{Li}}^{4+})$). However, the size of these clusters cannot be determined on the basis of our simulations.

There are independent experimental observations which may be interpreted in favor of stoichiometry-related defect clusters. The observed inhomogeneity of LiNbO_3 single crystals detected by TEM measurements (27) seems to agree with the proposition of extended intrinsic defect clusters. Support is also given by electron spin resonance (ESR) investigations of Nb^{4+} in electrochemically reduced LiNbO_3 . The defects could be assigned to $\text{Nb}_{\text{Li}}^{3+}$ antisites with associated defects on neighboring cation sites (28). Further, measurements of the ac-response of reduced, congruent LiNbO_3 proved these crystals to be highly inhomogeneous (29). The observed partition into insulating and conducting regions may be understood on the basis of extended stoichiometry-related defect clusters which contain Nb-antisite defects acting as electron traps. Therefore, the defect clusters would constitute the ac-conducting regions.

Anticipating the existence of stoichiometry-related defect clusters turns out to be important in order to properly understand the incorporation mechanisms of impurity ions such as magnesium. On the other hand, for present purposes the precise structure of these defect clusters is not relevant.

DISCUSSION OF MAGNESIUM SOLUTION MODELS

Subsequently I will discuss the Mg incorporation into Li_2O -deficient LiNbO_3 . The arguments, which are used to develop a consistent model, will be based on our earlier shell-model simulations (12, 13) and on experimental observations as the chemical analyses of Grabmaier *et al.* (30) and Iyi *et al.* (24). First, I emphasize that there are two distinct definitions in order to specify the Mg content in LiNbO_3 crystals:

$$c_{\text{Mg}}^{(1)} = \frac{[\text{MgO}]}{[\text{Li}_2\text{O}] + [\text{MgO}] + [\text{Nb}_2\text{O}_5]} \quad [5]$$

$$c_{\text{Mg}}^{(2)} = \frac{[\text{MgO}]}{[\text{LiNbO}_3] + [\text{MgO}]} \quad [6]$$

In what follows I use the first definition which is adapted to the $\text{Li}_2\text{O}\text{-MgO}\text{-Nb}_2\text{O}_5$ phase diagram. For moderate Mg concentrations the approximate relation between both definitions is given by $c_{\text{Mg}}^{(2)} \sim 2c_{\text{Mg}}^{(1)}$.

Before discussing the details of impurity solution mechanisms I compile some relevant experimental information which is related to the incorporation of extrinsic cations. All solution mechanisms suggested so far must be consistent with these experimental conditions in order to be realistic.

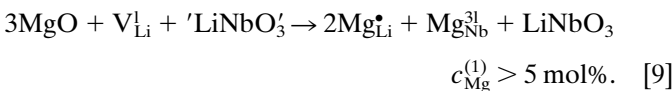
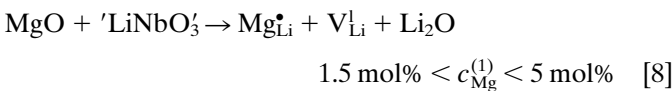
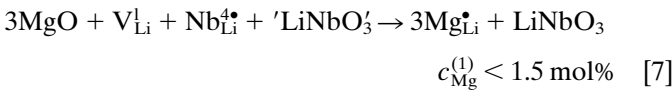
- The first observation concerns second harmonic generation (SHG) experiments on Mg-doped LiNbO_3 : The composition dependence of the SHG phase-matching tempera-

ture is significantly changed in vapor transport equilibrated (VTE) materials for Mg concentrations below the critical threshold value $c_{\text{Mg}}^{(1)} \sim 5$ mol% (31). There are no corresponding changes above the threshold. VTE treatments only affect Li-deficient LiNbO_3 with corresponding intrinsic defect structures. Thus, in $[\text{Li}]/[\text{Nb}]$ -congruent LiNbO_3 crystals stoichiometry-related defects (cation vacancies and Nb antisites) exist up to a Mg content of $c_{\text{Mg}}^{(1)} \sim 5$ mol%. They completely disappear for larger Mg concentrations.

- Second, consistent with these SHG investigations the recent ESR and optical absorption experiments on Mg-, Zn-, In-, and Sc-doped LiNbO_3 prove the existence of (electrochemically reduced) Nb antisites for all impurity concentrations below the respective threshold values (32, 33); the antisites are absent above the threshold concentrations. It is noted that modest reduction treatments do not significantly change the antisite concentration. For divalent cations the threshold concentration has been determined to range between 5 and 7 mol%; the precise value depends on the particular impurity. For trivalent cations such as In^{3+} or Sc^{3+} the threshold concentration reduces to 1–2 mol%.

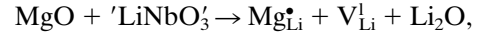
- The final observation relates to the concentration dependence $[\text{Li}] = f([\text{Mg}])$ as derived from the chemical composition analyses by Grabmaier *et al.* (30) and by Iyi *et al.* (24). Between about 1.5 mol% $< c_{\text{Mg}}^{(1)} < 5$ mol% the slope of this function $d[\text{Li}]/d[\text{Mg}]$ becomes close to -1 ; it is considerably less negative outside this range (see also Fig. 1).

Recently, Iyi *et al.* (24) proposed the following magnesium solution model which basically consists of the three subsequent incorporation reactions:

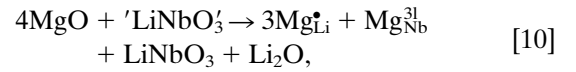


In this model no account has been made of possible defect clustering effects. Equation [7] predicts that all stoichiometry-related defects are completely consumed at $c_{\text{Mg}}^{(1)} = 1.5$ mol% magnesium. Iyi *et al.* use the Eqs. [7] and [8] in order to explain the observed change of slope of the function $[\text{Li}] = f([\text{Mg}])$ close to this Mg concentration. However, this interpretation contradicts those experimental observations which prove that stoichiometry-related defects, such as Nb antisites, exist up to a Mg content of about 5 mol%

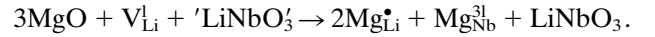
(see the first two items discussed above). A further inconsistency follows by considering our earlier shell-model simulations: Assuming hypothetically the validity of Eq. [7] up to a Mg content of 1.5 mol% one *must* next employ Eq. [8],



in order to explain the slope of the function $[\text{Li}] = f([\text{Mg}])$ close to -1 for 1.5 mol% $< c_{\text{Mg}}^{(1)} < 5$ mol% (30, 24). However, reaction [8] is energetically highly unfavorable in comparison with alternative incorporation reactions. Our previous simulations suggest that self-compensation-type solution modes would be significantly preferred,



which become even more favorable (by 0.6 eV per MgO) by taking advantage of existing Li vacancies. The resulting reaction corresponds to Eq. [9]:



Equation [10] is by 2 eV per MgO molecule more favorable than reaction [8]. Hence only a very small minority of magnesium cations can be incorporated into LiNbO_3 according to Eq. [8]; instead, the majority of the cations would be solved on the basis of self-compensation. Our previous simulations (13) have shown that self-compensation is the most favorable incorporation mode in the absence of stoichiometry-related defects. Thus, Eq. [7] would be followed by Eq. [10] for $c_{\text{Mg}}^{(1)} > 1.5$ mol%. Further support in favor of self-compensation is given by various independent theoretical and experimental investigations. First, the significance of these incorporation modes is not restricted to LiNbO_3 ; based on shell-model simulations these solution modes have also been predicted to be favorable in the related $A^{1+}B^{5+}O_3^{2-}$ perovskite materials such as KTaO_3 and KNbO_3 (16, 18). Even in $A^{2+}B^{4+}O_3^{2-}$ perovskites like BaTiO_3 (15) self-compensation may occur, but it is principally restricted to trivalent cations. In the particular case of LiNbO_3 further evidence is provided by the oxide $\text{Mg}_4\text{Nb}_2\text{O}_9$ which occurs in the Li_2O – MgO – Nb_2O_5 phase diagram for large MgO concentrations. The growth of this oxide from LiNbO_3 may easily be understood given the occurrence of self-compensation (13). Moreover, ESR experiments on $\text{LiNbO}_3:\text{Mg,Fe}$ ($c_{\text{Mg}}^{(1)} > 5$ mol%) have shown the existence of a second Fe^{3+} signal in addition to that usually observed which may be explained on the basis of self-compensation (34, 13). This interpretation has been supported by recent extended X-ray absorption fine-structure (EXAFS) measurements on $\text{LiNbO}_3:\text{Mg,Fe}$

(37). Finally, Malovichko *et al.* (38) identified $\text{Fe}_{\text{Li}}^{3+}$ and $\text{Fe}_{\text{Nb}}^{3+}$ defects in stoichiometric LiNbO_3 which agrees with the predictions of self-compensation type solution modes.

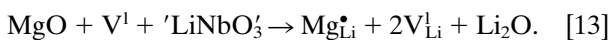
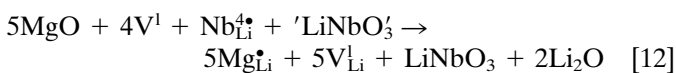
These brief remarks may be sufficient to demonstrate that in spite of its appealing simplicity the doping model of Iyi *et al.* (24) does not match the experimental and theoretical constraints. Most importantly, the observed change of slope close to 1.5 mol% cannot be simply related to a complete consumption of stoichiometry-related defects. Instead, it becomes obvious that at least two different incorporation reactions consuming stoichiometry-related defects are relevant for the solution of magnesium below 5 mol%. The change of slope at 1.5 mol% is then related to a change between these reactions. As will be argued below, such a change can easily be understood if one assumes the existence of stoichiometry-related defect clusters. On the other hand, in the case of isolated defects there is no obvious explanation for the change of slope.

The subsequent discussion essentially follows our earlier suggested incorporation mechanisms [13], but different from the original formulation I will now omit the precise structure of the stoichiometry-related vacancies in order to principally allow for both stoichiometry models (i.e., Eqs. [1] and [4]). Moreover, following the discussion in the preceding section the formation of extended stoichiometry-related defect clusters is in either model assumed to be energetically favorable. The stoichiometry-related cation vacancies, which are subsequently simply denoted as V^1 , form together with the existing Nb antisites the proposed defect clusters. These clusters consist of aggregations of the more basic ($4V^1\text{-Nb}_{\text{Li}}^{4+}$) units. The precise structure of these clusters is not important for present purposes, but it can be assumed that it is largely determined by the highly charged antisite defects. V_{Li}^1 , on the other hand, now denotes Li vacancies which are created during the Mg incorporation. These vacancies can be isolated point defects, but they may as well be associated with the Mg cations. Our previous model may now be generalized as follows:

- $c_{\text{Mg}}^{(1)} < 1.5 \text{ mol\%}$:



- $1.5 \text{ mol\%} < c_{\text{Mg}}^{(1)} < 5 \text{ mol\%}$:



- $c_{\text{Mg}}^{(1)} > 5 \text{ mol\%}$:

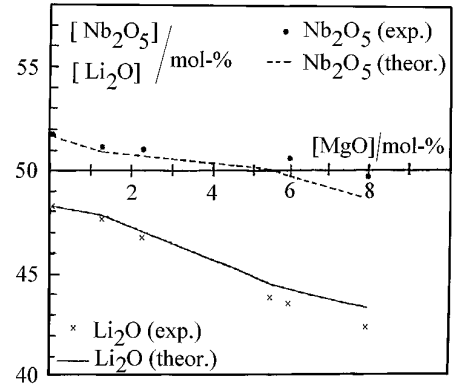
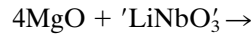
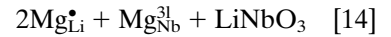
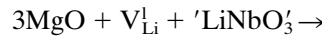
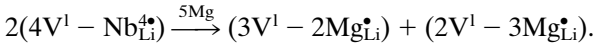


FIG. 1. Comparison of calculated and experimental Li_2O and Nb_2O_5 concentrations as a function of the MgO content. The results refer to congruent $[\text{Li}_2\text{O}]/[\text{Nb}_2\text{O}_5]$ melt compositions.



For small Mg concentrations reaction [11] has been found to represent the most favorable solution mode. This has been verified by approximating the occurring V^1 by ilmenite-type vacancies ($V_{\text{Nb}}^1\text{Nb}_{\text{Li}}^{4+}$) or by ordinary Li vacancies and even assuming basic aggregations between antisites and vacancies V^1 . Whereas below 1.5 mol% Nb antisites are preferentially consumed, this becomes true for V^1 in the regime $1.5 \text{ mol\%} < c_{\text{Mg}}^{(1)} < 5 \text{ mol\%}$. As will be argued below such a behavior can only be explained on the basis of suitable defect clusters. The proposed model is in agreement with the imposed experimental constraints, because stoichiometry-related defects exist up to the threshold Mg concentration of 5 mol%. Figure 1 compares the calculated and experimental Li_2O and Nb_2O_5 concentrations as a function of the MgO content. The results refer to otherwise congruent $[\text{Li}_2\text{O}]/[\text{Nb}_2\text{O}_5]$ melt compositions.

Let us now consider in some detail the relevant implications of stoichiometry-related defect clusters. The starting incorporation mode in our model is given by Eq. [11] which predicts a preferred consumption of Nb-antisite defects. According to Eq. [11], only two of five magnesium ions are able to replace Nb antisites. The remaining three Mg ions will likely occupy a corresponding number of vacancies V^1 . It is reasonable to assume that the incorporation of magnesium tends to keep the local accumulation of large excessive charges at a minimum. On the basis of Eq. [11] this may be accomplished by the formation of two singly charged subcomplexes:



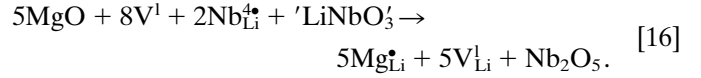
Based on the arguments in the preceding section we assume that the defect clusters in congruent $LiNbO_3$ are sufficiently extended and, therefore, stable in order to accommodate a certain concentration of these singly charged subcomplexes. However, with growing Mg content the whole intrinsic defect clusters are expected to become increasingly destabilized due to this charge imbalance. Consequently there should be a critical Mg concentration between 0 and 2.5 mol% at which other solution modes compensating for this charge imbalance become more favorable than Eq. [11].¹ We fitted the critical concentration to the reported change of slope at 1.5 mol%, since a theoretical prediction was impossible on the basis of our simulations. The critical Mg concentration $c_{Mg}^{(1)}(crit.) \sim 1.5$ mol% is significantly smaller than 2.5 mol% defining the upper limit for reaction [11]. Consequently, there remain sufficient stoichiometry-related defects which may be used to incorporate further magnesium cations. Between 1.5 mol% $< c_{Mg}^{(1)} < 5$ mol% our model suggests the combination of the solution modes [12]–[13]. Particularly reaction [13] may take advantage of the existing defect structures, because the newly created Mg_{Li}^{\bullet} and V_{Li}^1 defects can be favorably bound to the existing singly charged subcomplexes which are neutralized in this way. Further, with increasing Mg content it should become energetically favorable to reorganize the structure of the defect clusters by changing the V^1 to ordinary V_{Li}^1 which are more appropriate for the increasingly dominating Mg cations. During this process described by Eq. [12] an additional number of Li ions must be repelled from their original sites in order to maintain charge compensation. It is emphasized that the formation and distribution of V^1 vacancies essentially refers to the earlier existence of Nb antisites. As the divalent Mg cations certainly behave differently from the higher valent Nb antisites, a corresponding structural reorganization seems to be reasonable. On the other hand, if we assume the Li_2O -deficiency model [1] without any defect clusters, reaction [13] reduces to the unfavorable Eq. [8] which again would cause the problems discussed in connection with the model of Iyi.

On the basis of Eqs. [12]–[13] the threshold concentration close to 5 mol% is determined by the complete consumption of stoichiometry-related defects. The incorporation of additional magnesium (up to the observed magnesium solution limit) is finally predicted employing the self-compensation-type reactions [14]–[15].

The above discussion essentially hinges on the existence

¹ Assuming 1 mol% Nb antisites (possible antisites which are part of V^1 have been subtracted) corresponding to congruent $LiNbO_3$, reaction [11] allows the incorporation of $c_{Mg}^{(1)} = 2.5$ mol% magnesium.

of extended and stable defect clusters. If this assumption were wrong, reaction [11] should be rewritten as



In Eq. [16] we have retained the notation of V^1 vacancies to emphasize their stoichiometry-related origin, but these defects may be thought of simply representing ordinary Li vacancies. In this situation of predominantly isolated defects there would be no plausible reason to modify the solution mode up to complete consumption of the stoichiometry-related defects. Following Eq. [16] there are no stoichiometry-related defects beyond a Mg concentration of 2.5 mol%. Consequently, we would be left with similar inconsistencies as in the model of Iyi *et al.* discussed above.

However, reaction [16] may be relevant, if we consider near-stoichiometric $LiNbO_3$ instead of congruent crystals. The intrinsic defect clusters would consist of only a very few $(4V^1 - Nb_{Li}^{4\bullet})$ units and even the smallest Mg concentrations would significantly disturb the intrinsic defect structure; this situation can most easily be expressed on the basis of Eq. [16]. According to this equation impurity cations become effectively compensated by ordinary Li vacancies V_{Li}^1 . Electron nuclear double resonance (ENDOR) experiments for near-stoichiometric $LiNbO_3:Mn^{2+}$ (36), which indicate the presence of $Mn_{Li}^{\bullet} - V_{Li}^1$ aggregates, seem to be consistent with this interpretation. Most importantly, the existence of such aggregates does not require the energetically costly solution mode [8].

Finally, I briefly comment on the incorporation of trivalent impurity cations. As has been mentioned above the impurity threshold concentration occurs between 1 and 2 mol%. This result can be readily understood by considering the energetically most favorable solution reaction for trivalent cations such as indium In^{3+} (13):



On the basis of this reaction a maximal indium concentration of 1.67 mol% can be solved into congruent $LiNbO_3$. By comparison of Eqs. [11] and [17] it is obvious that trivalent impurity ions are more effective in consuming the Nb antisites than divalent cations, because the ratio of replacement is increased from 2:5 to 3:5. Further, due to their charge state trivalent cations may be expected to fit better with the intrinsic defect clusters than divalent cations. Based on these observations it is likely that the majority of the existing Nb antisites can be replaced by trivalent cations employing reaction [17] which would agree with the observed threshold behavior. On the other hand, the

greater charge misfit (with respect to Nb antisites) in the case of divalent cations causes a more pronounced destabilization of the stoichiometry-related defect clusters and, therefore, leads to the sequence of solution modes Eqs. [11]–[13] which predict the observable threshold phenomena to occur at 5 mol%.

CONCLUSIONS

In the present contribution the incorporation of magnesium into LiNbO_3 has been discussed. The arguments were based on our previous shell-model simulations. Different from the earlier discussion, however, no particular recourse has been made to the specific nature of stoichiometry-related cationic defect models, i.e., to the assumption of Li- or Nb-vacancy models. The present discussion demonstrates that a realistic magnesium solution model, which is in agreement with all experimental data, would be independent of these particular stoichiometry-related defects. It becomes clear, however, that defects resulting from Li_2O deficiency must form sufficiently extended clusters in order to accomplish a consistent magnesium solution model. Shell-model-based simulations suggest that a corresponding formation of defect clusters is favorable independent of the specific nature of the underlying Li_2O -deficiency model. The stability of these defect clusters upon the impurity incorporation seems to represent a key for a proper understanding of the cation solution.

ACKNOWLEDGMENTS

The financial support of this work by the Deutsche Forschungsgemeinschaft (SFB 225) is gratefully acknowledged. For many helpful discussions I am indebted to Professor O. F. Schirmer and to Professor M. Wöhlecke.

REFERENCES

1. Gi-Guo Zhong, Jin Jian, and Zhong-Kang Wu, in "Proceedings of the 11th International Quantum Electronics Conference." IEEE Cat. No. 80 CH1561-0, 631, 1980.
2. K. L. Sweeney, L. E. Halliburton, D. A. Bryan, R. R. Rice, R. Gerson, and H. E. Tomaschke, *J. Appl. Phys.* **57**, 1036 (1985).
3. F. Klose, M. Wöhlecke, and S. Kapphan, *Ferroelectrics* **92**, 181 (1989).
4. H. Fay, W. J. Alford, and H. M. Dess, *Appl. Phys. Lett.* **12**, 89 (1968).
5. F. A. Kröger and H. J. Vink, in "Solid State Physics" (F. Seitz and D. Turnbull, Eds.), Vol. 3. Academic Press, New York, 1956.
6. S. C. Abrahams and P. Marsh, *Acta Crystallogr. B* **42**, 61 (1986).
7. G. E. Peterson and A. Carnevale, *J. Chem. Phys.* **56**, 4848 (1972).
8. L. J. Hu, Y. H. Chang, I. N. Lin, and S. J. Yang, *J. Cryst. Growth* **114**, 191 (1991).
9. N. Iyi, K. Kitamura, F. Izumi, J. K. Yamamoto, T. Hayashi, H. Asano, and S. Kimura, *J. Solid State Chem.* **101**, 340 (1992).
10. A. P. Wilkinson, A. K. Cheetham, and R. H. Jarman, *J. Appl. Phys.* **74**, 3080 (1993).
11. J. Blümel, E. Born, and Th. Metzger, *J. Phys. Chem. Solids* **55**, 589 (1994).
12. H. Donnerberg, S. M. Tomlinson, C. R. Catlow, and O. F. Schirmer, *Phys. Rev. B* **40**, 11909 (1989).
13. H. Donnerberg, S. M. Tomlinson, C. R. Catlow, and O. F. Schirmer, *Phys. Rev. B* **44**, 4877 (1991).
14. C. R. A. Catlow and W. C. Mackrodt (Eds.), "Computer-Simulation of Solids," Lecture Notes in Physics, Vol. 166. Springer-Verlag, Berlin, 1982.
15. G. V. Lewis and C. R. A. Catlow, *J. Phys. Chem. Solids* **47**, 89 (1986).
16. M. Exner, Ph.D. Thesis, University of Osnabrück, 1993.
17. H. Donnerberg and M. Exner, *Phys. Rev. B* **49**, 3746 (1994).
18. M. Exner, H. Donnerberg, C. R. A. Catlow, and O. F. Schirmer, *Phys. Rev. B* **52**, 3930 (1995).
19. H. Donnerberg and C. R. A. Catlow, *J. Phys. Condens. Matter* **5**, 2947 (1993); H. Donnerberg and C. R. A. Catlow, *Phys. Rev. B* **50**, 744 (1994).
20. L. Schuh, R. Metselaar, and C. R. A. Catlow, *J. Eur. Ceram. Soc.* **7**, 67 (1991).
21. M. S. Islam, M. Leslie, S. M. Tomlinson, and C. R. A. Catlow, *J. Phys. C: Solid State Phys.* **21**, L109 (1988).
22. R. C. Baetzold, *Phys. Rev. B* **42**, 56 (1990).
23. J. H. Harding, *Rep. Prog. Phys.* **53**, 1403 (1990).
24. N. Iyi, K. Kitamura, Y. Yajima, and S. Kimura, *J. Solid State Chem.* **118**, 148 (1995).
25. D. M. Smyth, "Proceedings of the Sixth IEEE International Symposium on the Application of Ferroelectrics." June 1986.
26. A. Mehta, A. Navrotsky, N. Kumada, and N. Kinomura, *J. Solid State Chem.* **102**, 213 (1993).
27. M. E. Twigg, D. N. Maher, S. Nakahara, T. T. Sheng, and R. J. Holmes, *Appl. Phys. Lett.* **50**, 501 (1987).
28. H. Müller and O. F. Schirmer, *Ferroelectrics* **125**, 319 (1991).
29. K. Wulf, H. Müller, O. F. Schirmer, and B. C. Grabmaier, *Radiation Effects Defects Solids* **119–121**, 687 (1991).
30. B. C. Grabmaier, W. Wersing, and W. Koestler, *J. Cryst. Growth* **110**, 339 (1991).
31. U. Schlarb and K. Betzler, *Phys. Rev. B* **50**, 751 (1994).
32. T. Volk, M. Wöhlecke, N. Rubinina, N. V. Razumovski, F. Jermann, C. Fisher, and R. Böwer, *Appl. Phys. A* **60**, 217 (1995).
33. T. Volk, M. Wöhlecke, A. Reichert, F. Jermann, and N. Rubinina, *Ferroelectric Lett.* in press.
34. A. Böker, H. Donnerberg, and O. F. Schirmer, *J. Phys. Condens. Matter* **2**, 6865 (1990).
35. B. C. Grabmaier and F. Otto, *Proc. SPIE Int. Soc. Opt. Eng. (USA)* **651**, 2 (1986).
36. G. Corradi, H. Söthe, J.-M. Spaeth, and K. Polgar, *Radiation Effects Defects Solids* **119–121**, 583 (1991).
37. G. Corradi, A. V. Chadwick, A. R. West, K. Cruickshank, and M. Paul, EURODIM conference, Lyon, 1994.
38. G. I. Malovichko, V. G. Grachev, O. F. Schirmer, and B. Faust, *J. Phys. Condens. Matter* **5**, 3971 (1993).